WORLD CONFERENCE ON TIMBER ENGINEERING 2025
BRISBANE, AUSTRALIA
Advancing Timber for the Future Built Environment

CROSS-LAMINATED TIMBER WITH GAPS FOR WALL ELEMENTS

Kay Ackermann[1], Stefanie Christl[2], Philipp Dietsch[3]

ABSTRACT: Cross-laminated timber (CLT) is one of the most relevant modern mass-timber products with continuous growth in worldwide market share. The increased demand of CLT products, however, goes hand in hand with an increasing use of raw material. Among various approaches to optimize the use of timber, the reduction of material within the CLT layup is pursued in the work presented here. The objective is to decrease structural overperformance, which is evident within CLT wall elements where fire resistance is oftentimes the decisive design factor. Toward this aim, an experimental study was performed to examine the effects of CLT layups with gaps on mechanical properties. Tests on bending and buckling behavior as well as in-plane shear properties were performed. A variation of layups with different gap widths and lamination dimensions (75 mm, 95 mm, 115 mm) was investigated. This study shows that bending and buckling properties are strongly influenced by the reduced volume fraction in the layup. Increased shear deformation in the cross layers led to a decrease in load-carrying capacity and element stiffness. This showed signs of premature rolling shear failure. The evaluation of in-plane shear tests showed a much better correlation with the reduced net crossing-area between adjacent layers. Large gaps significantly influence the properties of CLT layups. In this study a material reduction up to 40 % was achieved, while sustaining considerable load-carrying capacity for the use of load-carrying wall elements.

KEYWORDS: cross-laminated timber, gaps, wall-elements, bending, buckling, in-plane shear, resource-efficiency

1 – INTRODUCTION

The fast-growing global market for mass timber structures involves a high demand for building products such as cross-laminated timber (CLT). This leads to an increasing consumption of sawn timber material. Despite industrial manufacturing methods and versatile applications CLT shows deficits in the (low) structural utilization of the material over the layup. This mainly applies to the inner cross and middle layer of the CLT layup of wall and floor elements. To increase resource and structural efficiency of wall elements a reduction of laminations within the CLT layup by creating gaps was studied. It is evident that large gaps in the layup are an effective method to reduce volume of high-quality timber. Those laminations can then be used in outer layers, where high strength is required. The aim of this study was to achieve a sustainable material reduction up to 30-40 % by varying geometric parameters such as gap-size and lamination dimensions. This triggered the questions of the impact on mechanical properties and the optimization of the layup regarding structural requirements of wall-elements. Further, the conducted investigations should close the knowledge gap of the structural behavior of in-plane loaded CLT wall elements with gaps, as recent studies focus on floor elements.

2 – BACKGROUND

Recent studies with large gaps primarily focused on experimental investigations of out-of-plane properties. The influence on bending and shear stiffness was further analyzed numerically [1]. It was shown that the reduced volume fraction leads to decreasing stiffness properties, mainly influenced by an increased shear deformation in the cross-layers [2]. To reinforce layups with large gaps, hardwood laminations from beech in inner layers was investigated [3]. It was concluded that beech laminations can improve the out-of-plane stiffness properties but not fully compensate the volume reduction. CLT with gaps also opens up possibilities towards multi-functional aspects, such as thermal activation [4], [5] and integration of gap fillings depending on desired function and utilization of the structural element. A state-of-the-art review on research developments of cross-laminated timber including large gaps is presented in [6].

3 – TEST SPECIMEN CONFIGURATIONS

3.1 MATERIAL AND ADHESIVE

The test specimens were produced from Norway spruce (*picea abies*) strength graded C24 according to EN 338 [7]. The laminations were not finger jointed. For gluing, a 1K-PUR was applied on each lamination before arrangement. The material properties were not specifically determined for each lamination beforehand. After performing the experimental tests, the raw density and moisture content (MC) was evaluated (see section 4).

3.2 DIMENSIONS AND LAYUPS

Five different layup configurations were produced. These include four layups with large gaps (75/1, 75/2, 95/1, 115/1) and one conventional CLT layup without intentional gaps, as reference series (75/0). The results of the layups with gaps are compared with the results from the reference series to allow a quantitative evaluation. The

[1] Kay Ackermann, KIT Timber Structures and Building Construction, Karlsruhe Institute of Technology, Karlsruhe, Germany, kay.ackermann@kit.edu

[2] Stefanie Christl, KIT Timber Structures and Building Construction, Karlsruhe Institute of Technology, Karlsruhe, Germany

[3] Philipp Dietsch, KIT Timber Structures and Building Construction, Karlsruhe Institute of Technology, Karlsruhe, Germany, dietsch@kit.edu, ORCID iD: 0000-0003-3568-8290

test specimens consist of five layers for all test series. Intentional gaps were introduced only to the middle and cross-layers. The outer layers remained homogeneously closed. The laminations in the reference cross-sections and outer layers with gaps were not edge glued. The gap-width w_{gap} was equal for all inner layers in parallel and cross direction. Further, w_{gap} coincides with the multiple of the board-width w_i used in an element. To describe the effect of gaps on the layup the following definition of the layer density δ_i was derived:

$$\delta_i = \frac{\sum w_i}{\sum(w_i + w_{gap})} \quad (1)$$

The layer density describes the remaining timber material in a single layer. Due to the double symmetric layup parallel layer 1 equals layer 5 and cross layer 2 equals layer 4. The material reduction in the layup can also be expressed by a gap-ratio. $\theta_{x,red}$ describes the reduced area in the cross-section, whereas $\theta_{y,red}$ expresses the reduction in the longitudinal direction. $\theta_{x,y,red}$ states the overall volume reduction in a layup according to (2). The same expression applies to the x- and y-direction by only respecting layers in the defined direction.

$$\theta_{x,y,red} = 1 - \frac{\sum \delta_i}{n} \cdot 100 \quad (2)$$

An overview of the relevant cross-section dimensions and projected gap-ratios of each series is given in Table 1. The given layer densities and gap-ratios are considered per meter.

Table 1. Dimensions and projected layup properties

Series		75/0	75/1	75/2	95/1	115/1
Layers n				5		
w_i [mm]		75	75	75	95	115
w_{gap} [mm] [1)]		0	75 (1)	150 (2)	95 (1)	115 (1)
t_i [mm]				20		
w_i / t_i		3.75	3.75	3.75	4.75	5.75
$\delta_1 = \delta_5$		1.00	1.00	1.00	1.00	1.00
$\delta_2 = \delta_4$		1.00	0.50	0.33	0.50	0.50
δ_3		1.00	0.50	0.33	0.50	0.50
gap-ratio [%] [2) 3)]	$\theta_{x,red}$	0	16.7	22.2	16.7	16.7
	$\theta_{y,red}$	0	50.0	66.7	50.0	50.0
	$\theta_{x,y,red}$	0	30.0	40.0	30.0	30.0

[1)] numbers in brackets state gap-size ratio w_{gap}/w_i

[2)] x-direction parallel layers (1, 3, 5) / y-diretction cross layers (2, 4)

[3)] x,y-direction refers to material reduction over volume per m³

It must be noted that small element widths have an influence on the projected gap-ratio and must hence be considered in the evaluation of test results. According to the lamination dimensions and gap-sizes given in Table 1, Fig. 1 shows the cross-sections of the investigated layups. The thickness of all layers was set to t_i = 20 mm resulting in an overall element thickness of t_{CLT} = 100 mm. Three different aspect-rations *w*/*t* were defined to evaluate its influence on the mechanical behavior. For better understanding of this influence, the gap-size ratio of series 75/1, 95/1 and 115/1 was set to w_{gap}/w_i = 1. To obtain bending failure in the four-point bending test and to prevent a premature shear failure at the supports, the respective specimens were modified with a support reinforcement (Fig. 2) of the cross-layers. Additional tests without support reinforcement were conducted for series 75/1 and 75/2. The specimens for buckling and in-plane shear test were produced without support reinforcement.

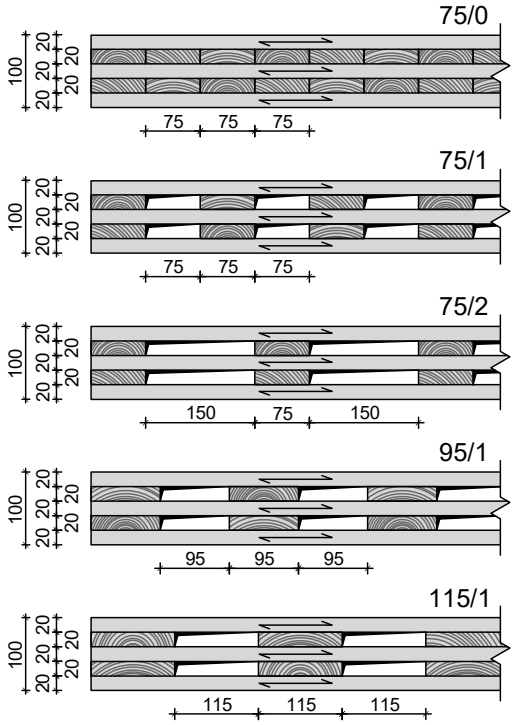

Figure 1. CLT layups with varying lamination dimensions and gap-sizes for the experimental campaign [mm]

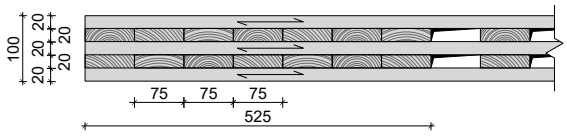

Figure 2. Support reinforcement of specimens for four-point bending tests (Series 75/1-SR) [mm]

The dimensions of the support reinforcement of each series and the adjusted volume reductions over the length are given in Table 2.

Table 2. Length of support reinforcement for bending tests

Series		75/0	75/1-SR	75/2-SR	95/1-SR	115/1-SR
l_{CLT} [mm]		2775	2775	2775	2755	2775
l_{sup} [mm]		-	525	525	475	525
l_{sup}/l_{CLT}		-	0.378	0.378	0.345	0.378
gap-ratio [%]	$\theta_{x,red}$	0	16.7	22.2	14.1	17.0
	$\theta_{y,red}$	0	49.8	66.4	49.8	49.8
	$\theta_{x,y,red}$	0	29.9	39.9	28.4	30.1

3.3 REMARKS ON SPECIMEN QUALITY

Before testing, the specimens were visually assessed in terms of defects and other geometrical offsets. Some deficits were present regarding intended gap-size w_{gap} (± 5 mm), element thickness t_{CLT} (max. 8 mm) and application of the adhesive, as shown below. Due to production tolerances, small unintentional gaps in the full layers were present. This especially applies to the reference series. These small gaps were regarded as tolerable.

Gluing

At some specimens of the series 75/2 and 95/1 offsets in the adhesive application were observed. This is shown in Fig. 3. This offset was a consequence of an unevenly distributed application of the adhesive. This could have an influence on the mechanical behavior of the respective specimens (see section 4.2).

Figure 3. Offset of adhesive application

Pressing

Larger gap-sizes are a sensitive topic regarding the magnitude of pressure applied during the pressing process. A few test specimens from series 75/2 showed reduced element thickness of about 92 mm instead of the intended 100 mm. An example is shown in Fig. 4.

Figure 4. Test specimen with reduced element thickness (75/2)

Severe lamination compression and fiber breakage can be observed at the edges of the lamination in the middle layer. Those specimens were only used in buckling tests.

4 – EXPERIMENTAL INVESTIGATIONS

4.1 GENERAL

The experimental investigations were conducted at the KIT Research Center for Steel, Timber and Masonry in Karlsruhe, Germany. The main objective of the experimental campaign was to investigate the influence of large gaps in CLT on relevant properties of wall-elements. This includes tests on the out-of-plane and in-plane properties. Table 3 lists the experimental tests that were and will be conducted.

Table 3. Status of experimental investigations

Experiments	processing status
Bending	✓
Buckling	✓
In-Plane Shear	✓
Longitudinal Shear	in preparation
Thermal Conductivity	in preparation

Before testing, the moisture content (MC) of each specimen was measured in a depth of 10 mm by ram in electrode measuring a MC of 10.4 ±2 %. After testing, kiln dry tests were carried out to determine the density distribution and MC. The given net density distribution refers to the net cross-section of the specimens, without considering the gaps. The gross density distribution respects gaps according to the projected volume reduction $\theta_{x,y,red}$ stated in Table 1. The results for each series are presented in Fig. 5.

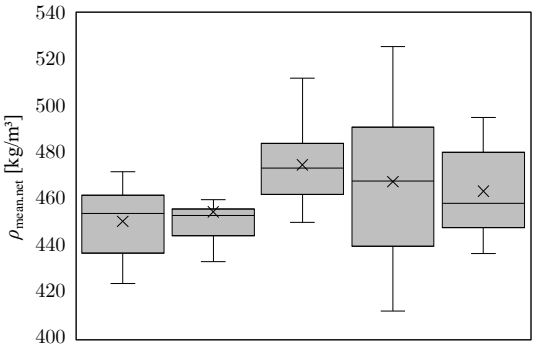

series	75/0	75/1	75/2	95/1	115/1
n [-]	14	17	16	14	13
$mean_{net}$ [kg/m³]	451.4	454.2	472.3	470.5	464.2
$mean_{gr}$ [kg/m³]	451.4	317.9	283.4	329.3	324.9
COV_{ρ} [%]	3.2	3.3	3.9	7.1	3.8
MC [%]	10.6	10.2	10.2	9.9	9.6
COV_{MC}[%]	4.6	2.2	1.7	4.8	2.3

Figure 5. Density distribution and moisture content of the test specimens per layup

4.2 BENDING

Experimental Setup and Procedure

To assess the effective strength and stiffness properties, four-point bending tests were conducted. The specimens were loaded in out-of-plane direction in a flatwise position (Fig. 7) with an approximate span-to-thickness-ratio of l/t_{CLT} = 27 according to EN 16351 [8].

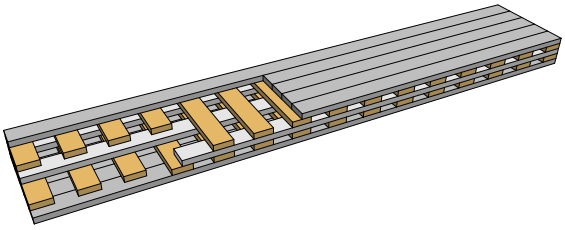

Figure 6. Specimen for bending tests with visualized gaps

Four tests per series were carried out. For the series 75/1 and 75/2 three additional tests without support reinforcement were performed. This should give an estimate of the influence of the support reinforcement on the load-carrying behavior of the specimens.

Table 4. Specimen dimensions for four-point bending test

Series	75/0	75/1	75/2	95/1	115/1
b_{CLT} [mm]			450		
t_{CLT} [mm]			100		
l_{CLT} [mm]	2775	2775	2775	2755	2775
$A_{x,net}$ [cm²]	270	225	210	232	224
$\theta_{x,red}$ [%]	0	16.7	22.2	14.1	17.0
$I_{y,net}$ [cm⁴]	2970	2955	2950	2957	2955
I_{gr}/I_{net}	0	0.0051	0.0067	0.0043	0.0052

The specimen dimensions are shown in Table 4, additionally stating the achieved cross-section reduction by the gaps in x-direction. This shows a slight deviation from the perceived reduction factor $\theta_{x,red}$ in series 95/1 and 115/1. Since the deviation results mainly from the reduction in the middle layer, the influence on the moment of inertia can be neglected (< 1 %).

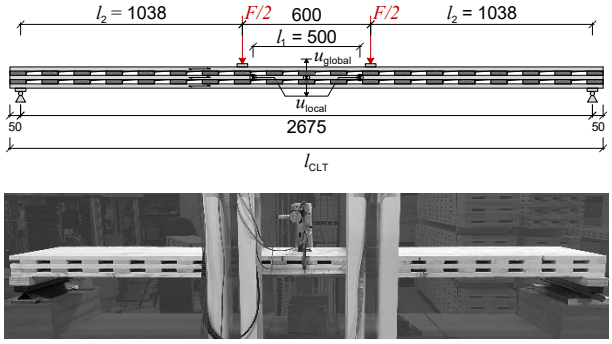

Figure 7. Four-point bending test setup (Series 75/1) [mm]

According to EN 16351, Annex C [8] and EN 408 [9] the effective stiffness properties of the layups were calculated considering a linear-elastic behavior between 0.1 F_{max} (F_1) and 0.4 F_{max} (F_2). Considering pure bending, the effective bending stiffness $EI_{local,net}$ is calculated respecting the local deflection u_{local}.

$$EI_{local,net} = \frac{l_2 \cdot l_1^2}{16} \cdot \frac{F_2 - F_1}{u_2 - u_1} = \frac{l_2 \cdot l_1^2}{16} \cdot \frac{\Delta F}{\Delta u_{local}} \quad (3)$$

According to EN 16351 [8] the effective shear stiffness (GA_{eff}) can be derived by performing a bending shear test, considering a span of l = 12 h. For comparative reasons, although the tests were realized with different l/h ratios, GA_{eff} was calculated as

$$GA_{eff} = \frac{24 \cdot EI_{local,net} \cdot EI_{global,net}}{(3 \cdot l^2 - 4 \cdot l_2^2) \cdot (EI_{local,net} - EI_{global,net})} \quad (4)$$

with the global effective bending stiffness $EI_{global,net}$ considering the global deflection u_{global} with

$$EI_{global,net} = \frac{3 \cdot l_2 \cdot l_{CLT}^2 - 4 \cdot l_2^3}{48} \cdot \frac{\Delta F}{\Delta u_{global}} \quad (5)$$

Failure Mechanism

Table 5 provides information about the observed failure mechanisms of each specimen. As expected, all reference specimens without gaps (75/0) failed due to bending failure in the lower outer layer. In series 75/1, 75/2 and 115/1 initial rolling shear failure in the cross-layers was predominant, which was not expected for the predefined specimen dimensions. Series 95/1 failed due to initial bending failure in most cases. Only a few specimens failed in a single failure mechanism. Specimens with support reinforcement showed initial rolling shear failure but did not fully collapse until longitudinal shear failure appeared in the middle layer. This led to a further increase of the maximum failure load.

Series 75/2 and 95/1 showed insufficient adhesive application at the cross-layers. The affected specimens were closely observed during experimental testing showing, that lamination failure in the glue-line did not cause initial specimen failure. Initial cracking occurred at load-states ≥ 0.6 F_{max}. This means, the obtained data can still be used for the evaluation of the bending and shear stiffnesses of the layups.

Table 5. Failure mechanism for each specimen in bending test

Series	supp. reinf.	F_{max} [kN]	failure mechanism [1)] b	r	l	d
75/0-1		48.90	**x**			
75/0-2		61.71	**x**			
75/0-3		57.21	**x**			
75/0-4		55.25	**x**			
75/1-1	x	40.10	x	**x**		
75/1-2	x	43.46	**x**	x	x	
75/1-3	x	36.87		**x**	x	
75/1-4	x	38.67		**x**	x	
75/1-5		33.14		**x**		
75/1-6		38.58	**x**			
75/1-7		31.14	x	**x**		
75/2-1	x	18.37		**x**	x	x
75/2-2	x	20.87		**x**	x	
75/2-3	x	17.40		**x**	x	
75/2-4	x	23.82		**x**	x	
75/2-5		16.65		**x**		
75/2-6		17.10		**x**		
75/2-7		15.25		**x**		x
95/1-1	x	36.87	x	**x**	x	
95/1-2	x	33.90	**x**			
95/1-3	x	35.91	**x**	x	x	
95/1-4	x	38.44	**x**			
115/1-1	x	37.22		**x**	x	
115/1-2	x	36.81		**x**	x	
115/1-3	x	33.74			**x**	
115/1-4	x	33.20	**x**	x	x	

[1)] initial failure mechanism highlighted
b = bending failure; r = rolling shear failure;
l = longitudinal shear failure at supp. reinf.;
d = bond line failure

Results and Discussion

The bending strength was not evaluated in this study, as in most cases shear failure was the predominant failure mechanism. If the failure loads were to be used to determine the bending strength for the net cross-section of series 75/0 and 95/1, the resulting values would be 48.7 N/mm² (COV = 9.5) and 31.8 N/mm² (5.2) respectively. Since F_{max} was strongly influenced by the support reinforcement, calculating the rolling shear strength would lead to false results. The effective rolling shear capacity could still be determined from the tests with rolling shear as sole failure mechanism. For the series 75/1, 75/1-SR, 75/2 and 75/2-SR the calculated effective rolling shear capacity would be 0.69 N/mm² (11.2), 0.8 N/mm² (7.0) and 0.33 N/mm² (5.7), 0.4 N/mm² (14.3) respectively. When considering an effective shear strength at the support reinforcement, the effective shear strength for series 75/1-SR and 75/2-SR would be 1.33 N/mm² and 0.67 N/mm² respectively.

The reduction of laminations in the cross-layer results in a reduced maximum load-carrying capacity (Fig. 8). This behavior correlates well with the perceived volume reduction in the layup (acc. Table 1 and Table 2) of series with $w_{gap}/w_i = 1$. By comparing series 75/1 and 75/2 with the reference series with support reinforcement a slight improvement of the load-carrying capacity can be achieved.

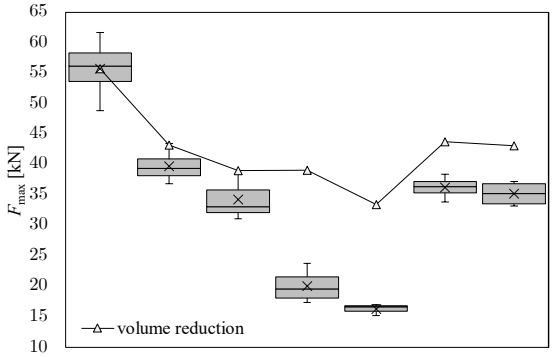

series	75/0	75/1-SR	75/1	75/2-SR	75/2	95/1-SR	115/1-SR
n [-]	4	4	3	4	3	4	4
mean [kN]	55.76	39.77	34.29	20.11	16.30	36.28	35.24
COV [%]	8.3	6.1	9.2	12.4	4.7	4.5	5.1

Figure 8. Maximum loads determined by experimental investigations including reduced volume ratio $\theta_{x,y,red}$

Series 75/2 shows a significantly lower load-carrying capacity relative to the volume reduction. This could primarily be caused by the decrease in rolling shear strength and a simultaneously non-linear increase in secondary stresses at the cross-lamination boundaries, as described in [10].

Series 75/1-SR, 95/1-SR and 115/1-SR show similar load-carrying capacities. The slight decrease of about 9 % for 95/1-SR and 11 % for 115/1-SR compared to series 75/1-SR could be due to the slight decrease in gap-size. The slight increase in load-carrying capacity between reinforced and unreinforced series could be a consequence of increased shear strength at the supports and the subsequent longitudinal shear failure in the middle layer.

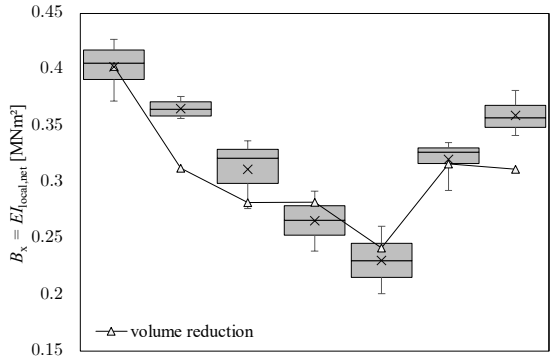

series	75/0	75/1-SR	75/1	75/2-SR	75/2	95/1-SR	115/1-SR
n [-]	4	4	3	4	3	4	4
mean [MNm²]	0.403	0.366	0.312	0.266	0.231	0.320	0.360
COV [%]	5.1	2.1	8.2	7.4	10.6	5.1	4.2

Figure 9. Local bending stiffness $EI_{local,net}$ from bending tests including reduced volume ratio $\theta_{x,y,red}$

Also the effective bending stiffness $EI_{local,net}$ is strongly influenced by the reduction of layer density (Fig. 9). Moreover, the calculated mean values show an approximate correlation to the volume reduction. Since the bending stiffness largely depends on the moment of inertia of the parallel outer layers, the decrease in stiffness should be less significant. This illustrates a substantial influence of the reduced cross-layer density. The support reinforcement increases the effective bending stiffness, which also shows that the restricted shear deformation of the cross-layers influences the bending stiffness.

In Fig. 10 an approximate convergence of the effective shear stiffness GA_{eff} and the volume reduction can be seen. This could be true due to the higher ratio of reduced cross-layer density in relation to the overall volume reduction. Both series 75/2 show a high COV. This could be due to deficiencies in the adhesive application and therefore increased but variable to stress redistributions. As beforementioned, the support reinforcement also affects the effective shear stiffness GA_{eff}.

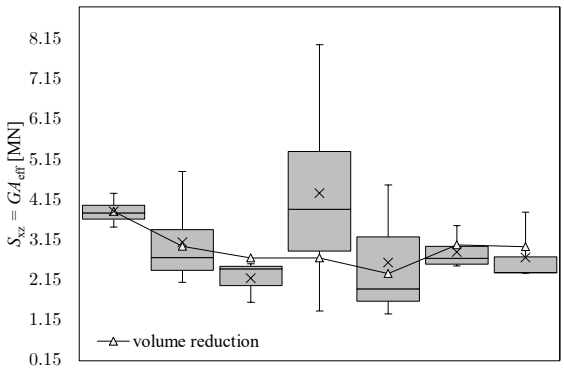

series	75/0	75/1-SR	75/1	75/2-SR	75/2	95/1-SR	115/1-SR
n [-]	4	4	3	4	3	4	4
mean [MN]	3.878	3.111	2.211	4.331	2.605	2.866	2.732
COV [%]	7.9	34.2	19.3	55.8	53.6	13.9	23.9

Figure 10. Effective shear stiffness GA_{eff} from bending tests including reduced volume ratio $\theta_{x,y,red}$

From a theoretical point of view, the reduction in shear stiffness should lead to an increase in bending stresses [11]. Following this argumentation, bending failure should be the predominant failure mode. It appears that the effect of the reduced shear stiffness on the bending stiffness is even larger. Before exceeding the maximum bending strength, premature rolling shear failure in the cross-layers appears.

4.3 BUCKLING

Experimental Setup and Procedure

Despite building physics and fire resistance aspects, member buckling verification is mostly decisive for wall elements. This especially applies to slender wall elements. Therefore, the buckling behavior was investigated by experimental buckling tests. The load was applied force-controlled at the top end of the specimen. At both ends of the specimen pinned supports are applied allowing free rotation, see Fig. 11.Four tests per series were carried out, except for series 75/2, where only 3 could be realized, due to a damage on the specimen. The buckling length l_{ef} equals the specimen length plus the height of the pinned supports. Due to the maximum machine load of 400 kN the specimen width b_{CLT} of series 75/0 had to be reduced according to Table 6. For better comparability of series 75/0, the results were recalculated to represent a specimen width of 300 mm. In general, the slenderness decreases slightly due to the reduction of area in the cross-section.

Table 6. Overview of specimen cross-section dimensions and gap-ratio of layups with gaps for buckling tests

Series	75/0	75/1	75/2	95/1	115/1
b_{CLT} [mm]	300		300		
t_{CLT} [mm]			100		
$l = l_{ef}$ [mm] [1)]			2885		
$A_{x,net}$ [cm²]	180	150	135	142	143
$\theta_{x,red}$ [%]	0	16.7	25.0	21.1	20.6
$\theta_{x,y,red}$ [%]	0	30.0	41.7	32.7	32.3
$I_{y,net}$ [cm⁴]	1980	1970	1965	1967	1968
i_y [mm]	33.17	36.24	38.15	37.22	37.09
λ	87.0	79.6	75.6	77.5	77.8

[1)] element length l_{CLT} + hinges

Further, due to the reduction of element width, a slight deviation results from the perceived reduction factor $\theta_{x,red}$ in series 95/1 and 115/1. Since the deviation is mainly a result of the reduction in the middle layer, the influence on the slenderness can be neglected (< 2.5 %).

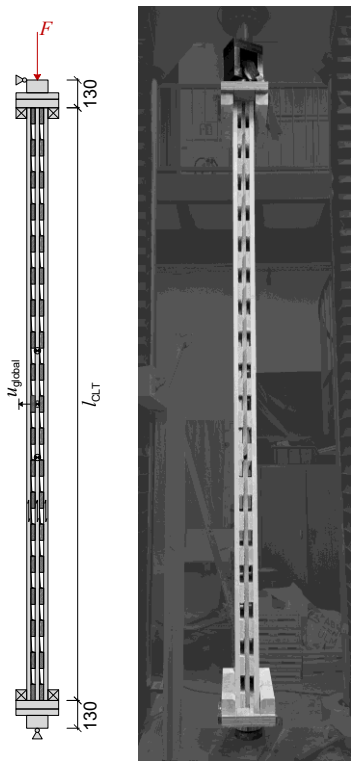

Figure 11. Buckling test setup for CLT wall elements with gaps [mm]

Failure Modes

All specimens failed due to buckling. This failure led to different secondary failure modes depending on the layup. Specimens of the reference series 75/0 encountered compression or bending failure at the outer layers. Series with gaps showed rolling shear failure in the cross-layers in almost all tests. This is a result of the extensive shear deformation of the layup due to the buckling deformation. Some specimens of series 75/2 experienced longitudinal shear failure in the middle layer. Despite extensive compression of some specimens during production, observed failure did not show signs of a related influence. Consequently, the obtained data will be used for the evaluation of test results

Results and Discussion

The maximum buckling loads for all tested series are shown in Fig. 12. It becomes evident that the introduction of large gaps has a significant influence on the load-carrying capacity of vertical loaded elements. Further, the variation of the gap-size ratio w_{gap}/w_i leads to considerable changes in load-carrying capacity. A gap-size ratio $w_{gap}/w_i = 1$ led to a decrease of about 30 % whereas a $w_{gap}/w_i = 2$ led to a decrease of about 61%.

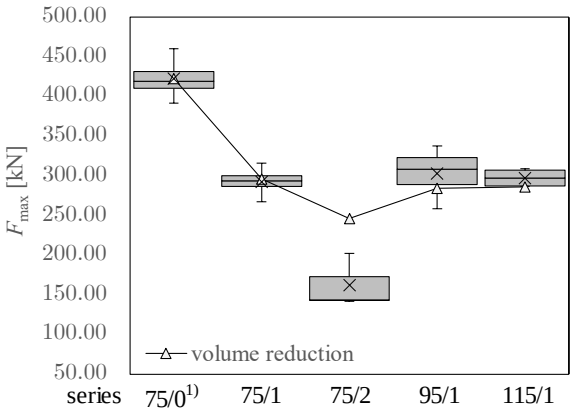

series	75/0[1)]	75/1	75/2	95/1	115/1
n [-]	4	4	3	4	4
mean [kN]	422.88	292.87	162.63	303.34	297.49
COV [%]	5.8	5.9	18.1	9.7	3.4

[1)] Recalculated from 250 mm to 300 mm

Figure 12. Buckling loads determined by experimental testing including reduced volume ratio $\theta_{x,y,red}$

When comparing series 75/1, 95/1 and 115/1 with a variation of the aspect-ratio of laminations w_i/t_i the difference in load-carrying capacity was small. Consequently, the variation of w_i/t_i with the respective lamination width has no further influence on the load-carrying capacity. This also correlates well with the obtained volume reduction. Further evaluation regarding the strength and stiffness of layups with gaps will be realized to better understand the buckling behaviour.

4.4 IN-PLANE SHEAR

Experimental Setup and Procedure

To determine the mechanical behavior of wall elements loaded in-plane , such as diaphragms, in-plane shear tests according to Kreuzinger & Sieder [12] were conducted.

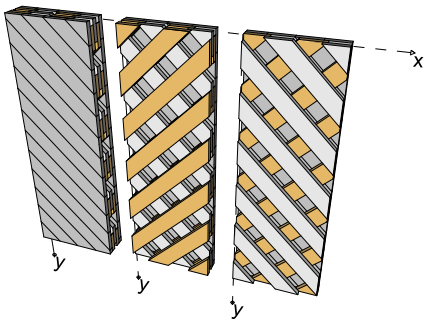

Figure 13. Specimen for in-plane shear tests with visualized gaps

The test setup proposes specimen dimensions of $h_{CLT}/w_{CLT} = 3$ with layer orientation rotated by 45°. The setup results in an approximately constant shear stress distribution in the middle third of the specimen.

Following EN 408 [9] the shear modulus was evaluated to investigate the stiffness behavior of the produced elements. The local shear deformation can be measured by a shear field (Fig. 14), which was conducted by 3D digital-image-correlation method (3D-DIC). Therefore, on each measuring point a small sticker with a speckle pattern was applied on both side faces of the specimens. Dual cameras on both sides track the movement of each point. This data can then be used to calculate the relative deformation of the shear field.

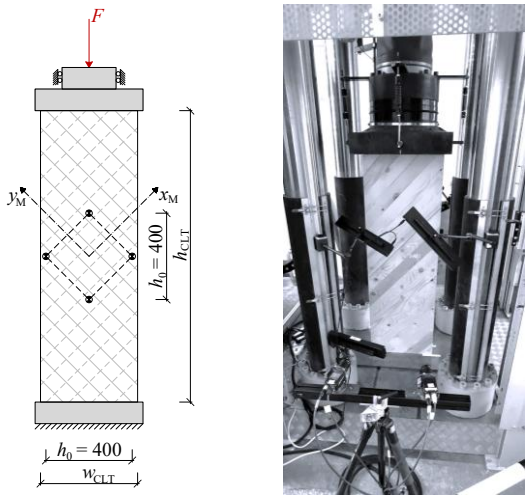

Figure 14. Experimental setup for in-plane shear tests [mm]

Six tests per series were conducted. Due to measuring errors of the local deformation, the available data of some series was reduced. Two specimens of series 75/2, 95/1 and 115/1 had small gaps (gr) of $w_{gap,out}$ = 5 mm in the outer layers to eliminate friction between adjacent laminations. The specimen dimensions are shown in Table 7.

Table 7. Specimen dimensions for in-plane shear tests

Series	75/0	75/1	75/2	95/1	115/1
b_{CLT} [mm]		450		435	450
h_{CLT} [mm]		1350		1310	1350
t_{CLT} [mm]			100		
$t_{eff,CLT}$ [mm]	100	70	60	70	70

One approach to take into account the effect of gaps in the inner layers of the layup and to be able to quantitively compare the stiffness in relation to CLT an effective element thickness $t_{eff,CLT}$ must be determined. The effective element thickness for each test series is given in Table 7.

$$t_{eff,CLT} = \sum t_i \cdot \delta_i \quad (6)$$

The shear modulus, can then be calculated from experimental results according to EN 408 [9] as shown by Silly [13]. By implementing the effective thickness $t_{eff,CLT}$, an effective shear modulus $G_{xy,eff}$, that accounts for the reduced volume fraction in the layup, can be derived by

$$G_{xy,eff} = \alpha_G \cdot \frac{h_0}{2 \cdot w_{CLT} \cdot t_{eff,CLT}} \cdot \frac{\Delta F}{\Delta w_G} \quad (7)$$

with $\Delta F/\Delta w_G$ as relation between applied load and shear deformation from horizontal and vertical displacement, determined in the linear elastic range between 0.1 and 0.4 F_{max} and h_0 as the size of the shear field.

The factor α_G defines a shear correction factor that adjusts measured deformations according to theoretical shear stress distribution in the shear field. From Brandner & Dietsch et al. [14] the correction factor can be assumed α_G = 1.0, as the difference between theoretical and real stress distributions are negligible. This must be further evaluated for the specific geometric and stiffness ratios (D_y/D_x = 2.5) of this series.

Failure Modes

In the reference series net-shear failure in the laminations was observed as main failure mechanism. This was the expected failure mode since the laminations were not edge-glued, which could have resulted in shear failure in the gross-cross-section according to [15]. In all series with gaps in the inner layers, torsional shear failure at the remaining crossing-areas of adjacent inner layers was observed. Most predominantly, this appeared between layers 2-3 or 3-4, due to the significantly reduced glued surface in those layers. Observations show that torsional shear strength is governed by rolling shear stresses, leading to rolling shear failure.

Results and Discussion

The evaluation of the maximum force on the tested specimens shows a significant decrease in in-plane load-carrying capacity, which can be seen in Fig. 15. The net crossing area in the layup was set in relation to the maximum load-carrying capacity.

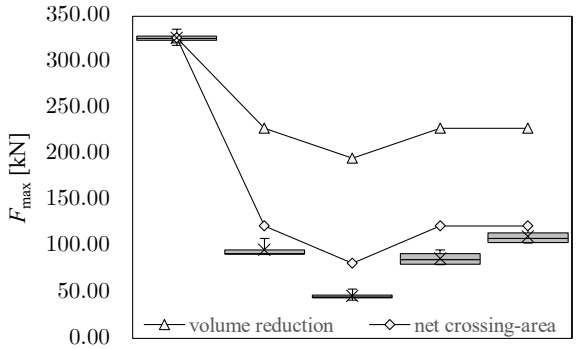

series	75/0	75/1	75/2	95/1	115/1
n [-]	4	4	6	6	5
mean [kN]	326.53	96.06	46.27	86.96	110.83
COV [%]	1.9	7.6	8.1	7.4	6.0

Figure 15. Maximum loads of in-plane shear tests including reduced volume ratio $\theta_{x,y,red}$

This shows a good correlation, indicating a significant influence of the net crossing-area on the load-carrying capacity of the layup. This corresponds to the observed failure mechanisms during the experimental study, as torsional shear failure in the crossing areas was predominant.

The calculated shear modulus according to (7) for each series is shown in Fig. 16. The mentioned relation to the net crossing-area can also be observed in the evaluation of the effective shear modulus. This is relevant for further evaluation of the in-plane shear properties of CLT with gaps.

From Fig. 15 and Fig. 16 it can also be taken that a linear relation between the reduction of the crossing-area to the load-carrying capacity and stiffness is present. When comparing the series with $w_{gap}/w_i = 1$ an increase in stiffness can be seen with increasing lamination width and consequently larger dimensions of crossing areas. Additional small gaps in the outer layers have a slight influence on the element stiffness. To further validate the observed tendencies further tests with larger lamination widths are encouraged.

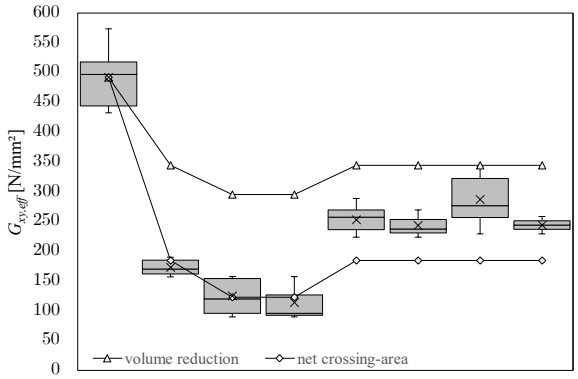

series	75/0	75/1	75/2	75/2gr	95/1	95/1gr	115/1	115/1gr
n [-]	6	7	9	3	9	3	9	2
mean [kN]	492.1	173.2	125.2	114.5	253.0	243.7	287.1	244.1
COV [%]	10.2	7.4	21.4	26.9	8.1	7.8	13.2	6.0

Figure 16. In-plane shear modulus including volume ratio $\theta_{xy,red}$

To validate the obtained results, two alternative approaches to calculate the shear modulus were used. The approach according to Kreuzinger & Sieder [12] determines the shear modulus based on the stiffness matrix for the state of plane stress and its transformation resulting in

$$G_{\mathrm{xM,yM}} = \frac{1}{\left(\frac{4}{E_{\mathrm{y}}} - \frac{1}{E_{\mathrm{xM}}} - \frac{1}{E_{\mathrm{yM}}}\right)} \tag{9}$$

The shear modulus is calculated as a function of the MOE of the material used for laminations in the transformed x_M- and y_M-direction (E_{xM} and E_{yM}) and the MOE of the test specimen in vertical direction determined from local vertical deformation measured during the experiment (E_y) with

$$E_{\mathrm{y}} = \frac{\Delta\sigma}{\Delta\epsilon} \tag{10}$$

Hereby, deformations and calculated stresses and strains are also evaluated in the linear elastic range between 0.1 and 0.4 F_{max}.

An alternative method is developed by Bogensperger et al. [16]. A theoretical approach to estimate the effective shear modulus based on shear failure mechanism in the crossing-areas is suggested. This approach is also given in EN 408 [8]. It can be calculated according to

$$G_{\mathrm{xy,EN}} = \frac{G_{\mathrm{0,l,mean}}}{1 + 6 \cdot \alpha_{\mathrm{T}} \cdot \left(\frac{t_{\mathrm{l,mean}}}{w_{\mathrm{i}}}\right)^2} \tag{11}$$

with

$$\alpha_{\mathrm{T}} = 0{,}43 \cdot \left(\frac{t_{\mathrm{l,mean}}}{w_{\mathrm{i}}}\right)^{-0{,}79} \tag{12}$$

for a 5-layer layup, with $G_{0,l,mean}$ as average shear modulus of the laminations and $t_{l,mean}$ as average layer thickness. As the same material and layer thickness is used for all series, the respective volume fraction needs to be considered to calculate the mean values. The results are shown in Fig. 17.

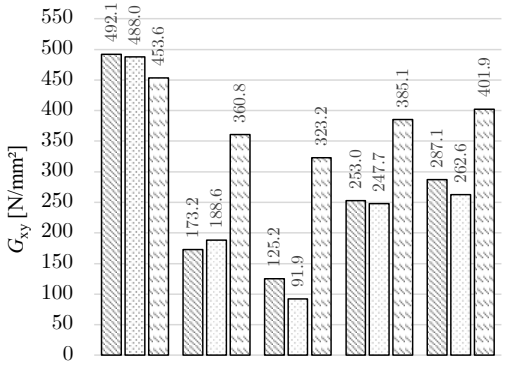

series	75/0	75/1	75/2	95/1	115/1
$G_{xy,eff}$ [N/mm²]	492.1	173.2	125.2	253.0	287.1
G_{xMyM} [N/mm²]	488.0	188.6	91.9	247.7	262.6
$G_{xy,EN}$ [N/mm²]	453.6	360.8	323.2	385.1	401.9

Figure 17. Comparison of experimental and theoretical investigations on in-plane shear modulus (each series from left to right: $G_{xy,eff}$, G_{xMyM}, $G_{xy,EN}$)

The method stated in (9) according to [12] shows shear moduli G_{xMyM} similar to the approach stated in (7), as both methods are based on experimental results. From [14] it is known that the results according (7) have a higher accuracy due to lower COVs, which can be confirmed for this study.

When comparing the experimental results with theoretically obtained values for $G_{xy,EN}$ according to Bogensperger, the shear modulus is largely overestimated. This may result from the sole consideration of the reduced volume in the layup, which underestimates the reduction of glued crossing-areas between layers.

5 – CONCLUSIONS

The influence of large gaps in CLT for wall elements was investigated. To determine the effect of different gap sizes and lamination dimensions on the mechanical properties, series of experimental tests were conducted. These included four-point bending, buckling and in-plane shear tests. During the bending tests, rolling shear failure in the crosslayers was predominant despite expected bending failure for the specimen dimensions studied. Consequently, the bending strength of the layups with large gaps could not be obtained. In contrast, this behavior showed that the element rolling shear capacity is significantly reduced. Moreover, the influence of the increased shear deformation in cross-layers has a significant influence on the bending properties.

The evaluation of the buckling tests demonstrates that the reduction in capacity has a high correlation with the reduced volume fraction. The reduction of laminations in the middle layer arranged in longitudinal direction weak correlation to the load-carrying capacity. The evaluation of in-plane shear tests was conducted according to Kreuzinger. These tests indicate a significant decrease in

load-carrying capacity and shear stiffness. Series 75/2 with a ratio $w_{gap}/w_i = 2$ reached a maximum decrease of up to 75 %. The minimum decrease was set by series 115/1 of about 42 % compared to the reference series 75/0. The average reduction of in-plane shear stiffness over all series with gaps is about 60 %. This decrease was mainly caused by a reduction in crossing area of adjacent layers. The comparison of experimental results with alternative theoretical method shows deficiencies of the alternative method (EN 408 [9]) in the estimate of the shear modulus.

Future investigations should focus on the influence of the reduced out-of-plane shear stiffness in cross-layers on the out-of-plane strength properties. The development of analytical approaches to estimate the buckling capacity is also required. It is encouraged to further study the influence of the failure mechanisms on in-plane shear capacity. Further, a stable design approach that considers the present gaps must be derived. This could be realized by further experimental testing on small scale specimens or numerical studies.

The manufacturer faced challenges during production of elements with large gaps, such as exceeded compression strength during pressing of the elements and offsets in adhesive application. Consequently, production processes need to be adjusted for better product quality. Additional tests will be performed on specimens manufactured with adjusted production settings.

Layups with gaps present resource efficient and lightweight elements. From this study it is shown that material reductions up to 40 % can be achieved. Even though the reduction in load-carrying capacity of wall elements is considerable, the remaining cross-section will still have acceptable load-carrying capacity for many applications, such as story additions for urban densification. Additionally, depending on the size of the design load the layup can be adjusted resulting in a tailored element for the specified application.

6 – ACKNOWLEDGEMENTS

The research project is funded by the German Federal Ministry of Education and Research (BMBF) in the course of Bioeconomy in the North project InnoTLT. Material and test specimens for the experimental campaign were produced by Lignotrend Produktions GmbH.

7 – REFERENCES

[1] L. Franzoni, A. Lebée, F. Lyon, and G. Forêt, “Elastic behavior of Cross Laminated Timber and timber panels with regular gaps: Thick-plate modelling and experimental validation,” *Engineering Structures*, vol. 141, pp. 402–416, 2018.

[2] L. Franzoni, A. Lebée, L. Florent, and G. Foret, “Bending behavior of regularly spaced CLT panels,” *14th World Conference on Timber Engineering (WCTE)*: Vienna, Austria, 2016.

[3] L. Bienert, N. Schumacher, S. Winter, and K. Richter, “Development of Disintegrated Hybrid Cross Laminated Timber,” *ICEM 2023*, pp. 943-954, Porto, Portugal, 2023.

[4] M. Arnold, P. Dietsch, and S. Winter, “Mechanical Properties of Innovative Multifunctional Cross-Laminated Timber,” *16th World Conference on Timber Engineering WCTE*: Santiago, Chile, 2020/21.

[5] K. Mindrup and S. Winter, “Thermal activation of solid timber elements for indoor climate control,” *15th World Conference on Timber Engineering (WCTE): Seoul, South Korea*, 2018.

[6] E. Serrano, Kay Ackermann, P. Dietsch, J. Haddal Mork, "Recent Developments on Tailored Laminated Timber," *18th World Conference on Timber Engineering (WCTE)*: Brisbane, Australia, 2025.

[7] *EN 338:2016-07, Structural timber - Strength classes*, European Committee for Standardization: Brussels, Belgium, 2016.

[8] *EN 16351:2021-06, Timber structures - Cross laminated timber - Requirements*, European Committee for Standardization: Brussels, Belgium, 2021.

[9] *EN 408:2012-10, Timber structures - Structural timber and glued laminated timber - Determination of some physical and mechanical properties*, European Committee for Standardization: Brussels, Belgium, 2012.

[10] T. Ehrhart and R. Brandner, “Rolling shear: Test configurations and properties of some European soft- and hardwood species,” *Engineering Structures*, vol. 172, pp. 554–572, 2018.

[11] P. Mestek, H. Kreuzinger, and S. Winter, “Flächen aus Brettstapeln, Brettsperrholz und Verbundkonstruktionen.,” *Holzbau der Zukunft - Teilprojekt 15*, 2008.

[12] H. Kreuzinger and M. Sieder, “Einfaches Prüfverfahren zur Bewertung der Schubfestigkeit von Kreuzlagenholz/Brettsperrholz,” *Bautechnik*, vol. 90, no. 5, pp. 314–316, 2013.

[13] G. Silly, “Schubfestigkeit der BSP-Scheibe - numerische Untersuchung einer Prüfkonfiguration,” Graz, Austria: holz.bau forschungs gmbh TU Graz, 2014.

[14] R. Brandner, P. Dietsch, J. Dröscher, M. Schulte-Wrede, H. Kreuzinger, and M. Sieder, “Cross laminated timber (CLT) diaphragms under shear: Test configuration, properties and design,” *Construction and Building Materials*, vol. 147, pp. 312–327, 2017.

[15] M. Flaig and H. J. Blaß, “Shear strength and shear stiffness of CLT-beams loaded in plane,” *CIB-W18/46-12-3*, Vancouver, Canada: Timber Scientific Publishing, KIT Holzbau und Baukonstruktionen, 2013.

[16] T. Bogensperger, T. Moosbrugger, and G. Silly, “Verification of CLT-plates under loads in plane,” *11th World Conference on Timber Engineering WCTE*: Riva del Garda, Trento, Italy, 2010.